EARTHQUAKE ENGINEERING AND STRUCTURAL DYNAMICS
Earthquake Engng. Struct. Dyn. **27**, 1149–1164 (1998)

ROBUST CONTROLLER DESIGN FOR THE ACTIVE MASS DRIVER BENCHMARK PROBLEM

PETER M. YOUNG[1,*] AND BOGUSZ BIENKIEWICZ[2]

[1]*Department of Electrical Engineering, Colorado State University, Fort Collins, CO 80523, U.S.A.*
[2]*Department of Civil Engineering, Colorado State University, Fort Collins, CO 80523, U.S.A.*

SUMMARY

In this paper we develop a robust controller design for the Active Mass Driver (AMD) benchmark problem. The design process is based around the D–K iteration procedure for (complex) μ synthesis, together with a balanced truncation procedure to reduce the controller order. The final design is a third-order linear controller, which utilizes only four accelerometer measurements, and has desirable rolloff properties (i.e. small required bandwidth, and a high degree of robustness). Despite the simplicity of the controller, it is able to yield quite good performance, while using only modest control authority. © 1998 John Wiley & Sons, Ltd.

KEY WORDS: structural control; active; optimal; robust

1. INTRODUCTION

The Active Mass Driver (AMD) benchmark problem provides a fairly realistic testbed for the study of control algorithms applied to civil engineering structures. The problem is based on an experimental setup in the Structural Dynamics and Control/Earthquake Engineering Laboratory at the University of Notre Dame. The experiment consists of a three-storey test structure equipped with an active mass driver actuation system and accelerometer/displacement sensors. These are controlled by a DSP-based real-time digital feedback control system. A full description of the benchmark problem, including system models and design requirements/constraints, may be found in Reference 1 (see also the Web Site at http://www.nd.edu/~quake/). A very brief description is given in Section 3.

The control design approach we use here is based on the D–K Iteration procedure for μ synthesis. An overview of this approach is included in Section 4 to illustrate the application of this design procedure to controller synthesis. The specific application to the benchmark problem is covered in detail in Section 5, including the selection procedure for the design interconnection and the corresponding weighting functions.

The resulting controller, after some further simplifications/transformations, is evaluated using the benchmark criteria, and the results are discussed in Section 6. It is seen that this design approach offers a great deal of flexibility for exploiting the various tradeoffs inherent to such a problem (e.g. control authority versus structural vibration attenuation). Furthermore, we are able to provide a final design for the controller which is very simple, has excellent robustness properties, and delivers good performance for modest control effort.

* Correspondence to: Peter M. Young, Department of Electrical Engineering, Colorado State University, Fort Collins, CO 80523, U.S.A. E-mail: pmy@engr.colostate.edu

CCC 0098–8847/98/111149–16$17·50

Received 21 May 1997
Revised 22 November 1997

2. NOTATION AND DEFINITIONS

The notation used here is fairly standard. For any matrix (or vector), M, we denote the transpose by M^{T}, and the complex conjugate transpose by M^*. The largest singular value is denoted by $\bar{\sigma}(M)$. We denote the $k \times k$ identity matrix by I_k. Occasionally, we will drop the subscript from I, whence it denotes an identity matrix of the appropriate size (from context).

We define the field of complex numbers by $\mathscr{C}$, and define $\mathscr{RM}$ to be the space of real-rational proper transfer matrices. A state-space representation for a transfer matrix $\mathbf{P} \in \mathscr{RM}$ is denoted by

$$\mathbf{P} = \left[\begin{array}{c|c} A & B \\ \hline C & D \end{array}\right] \doteq C(sI - A)^{-1}B + D \tag{1}$$

and we will refer to such representations of elements of $\mathscr{RM}$ as state-space systems. We define $\mathscr{RH}_\infty$ to be the subspace of $\mathscr{RM}$ with elements analytic in $\mathrm{Re}(s) \geqslant 0$, also referred to as stable systems. Given a transfer matrix $\mathbf{P} \in \mathscr{RH}_\infty$ we denote its infinity norm by

$$\|\mathbf{P}\|_\infty \doteq \sup_{\omega \in \mathscr{R}} \bar{\sigma}(\mathbf{P}(\mathbf{j}\omega)) \tag{2}$$

The definition of the structured singular value, μ, is dependent upon the underlying block structure of the uncertainties, which is defined as follows. Suppose we have a matrix $M \in \mathscr{C}^{n \times n}$ and a non-negative integer $m \leqslant n$. Then the block structure $\mathscr{K}(m)$ is an m-tuple of positive integers

$$\mathscr{K} = (k_1, \ldots, k_m) \tag{3}$$

This m-tuple specifies the dimensions of the perturbation blocks, and we require $\sum_{i=1}^{m} k_i = n$ in order that these dimensions are compatible with M. This determines the set of allowable perturbations, namely define

$$X_{\mathscr{K}} = \{\Delta = \text{block diag}(\Delta_1^C, \ldots, \Delta_m^C) \colon \Delta_i^C \in \mathscr{C}^{k_i \times k_i}\} \tag{4}$$

Note that $X_{\mathscr{K}} \subset \mathscr{C}^{n \times n}$. All the machinery presented here is *easily* generalized to the case where the uncertainty blocks need not be square. In fact, allowing non-square blocks is often useful in practice (indeed we will use non-square blocks for the AMD problem). However, although this generalization adds little difficulty to the problem, it does makes the notation very cumbersome, and so, for clarity of exposition, we will present all the analysis/design tools in this paper for the set-up in equation (4).

It is also possible to extend these tools to handle more general uncertainty classes, which can include real parametric uncertainty. This leads to the so-called mixed (real and complex) μ problem. We will not use these results here, and so we restrict our attention to the more standard (complex) μ problem, but we refer the interested reader to References 2–5 and the references therein for an in-depth treatment of the mixed μ problem. The following definition is taken from Reference 6:

Definition 1 (Reference 6). The structured singular value, $\mu_{\mathscr{K}}(M)$, of a matrix $M \in \mathscr{C}^{n \times n}$ with respect to a block structure $\mathscr{K}(m)$ is defined as

$$\mu_{\mathscr{K}}(M) = \left(\min_{\Delta \in X_{\mathscr{K}}} \{\bar{\sigma}(\Delta) \colon \det(I - \Delta M) = 0\} \right)^{-1} \tag{5}$$

with $\mu_{\mathscr{K}}(M) = 0$ if no $\Delta \in X_{\mathscr{K}}$ solves $\det(I - \Delta M) = 0$.

In order to present the relevant theory we define the following set of block diagonal scaling matrices (which, like μ itself, depends on the underlying block structure).

$$\mathscr{D}_{\mathscr{K}} = \{\text{block diag}(d_1 I_{k_1}, \ldots, d_m I_{k_m}) \colon d_i \in \mathscr{C},\ d_i \neq 0\} \tag{6}$$

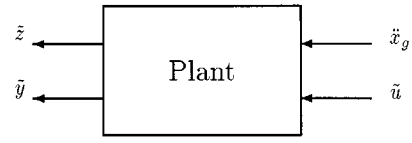

Figure 1. Benchmark problem open-loop plant model

3. THE ACTIVE MASS DRIVER BENCHMARK PROBLEM

The active mass driver benchmark problem is described in detail in Reference 1 (also see the Web Site at http://www.nd.edu/~quake/). The problem is based on an experimental setup in the Structural Dynamics and Control/Earthquake Engineering Laboratory at the University of Notre Dame, which consists of a three-storey single-bay structure which is equipped with an active mass driver (AMD) system, consisting of a single hydraulic actuator with an attached steel mass. The position of the mass is measured via a linear variable displacement transducer (LVDT) with a local position feedback control loop to stabilize the actuator. The LVDT position measurement is available for control purposes, along with 5 accelerometer measurements: one located on the actuator mass; one measuring the ground excitation; one on the floor of each bay of the structure (for a total of three). Additionally, five pseudo-velocity measurement are available, obtained by filtering the accelerometer measurements with approximate integrators. These measurements are fed back to a DSP-based real-time digital controller, which can then command the AMD system. The DSP controller utilizes A/D and D/A converters which have 12 bit precision, a span of ± 3 V, and operate at 1 kHz. The controller is limited to 12 states, with an associated computation delay of 200 μs. See Reference 1 for a detailed description of the experimental setup (including schematics and photographs).

Two models of this setup are provided in the benchmark problem, both of which correspond to Figure 1, where $\ddot{x}_g$ is the ground acceleration, $\tilde{u}$ is the (delayed) control signal, $\tilde{z}$ are the signals to be controlled, and $\tilde{y}$ are the measurements, namely:

$$\tilde{z} = (x_1 \;\; x_2 \;\; x_3 \;\; x_m \;\; \dot{x}_1 \;\; \dot{x}_2 \;\; \dot{x}_3 \;\; \dot{x}_m \;\; \ddot{x}_{a1} \;\; \ddot{x}_{a2} \;\; \ddot{x}_{a3} \;\; \ddot{x}_{am})^T$$
$$\tilde{y} = (x_m \;\; \ddot{x}_{a1} \;\; \ddot{x}_{a2} \;\; \ddot{x}_{a3} \;\; \ddot{x}_{am} \;\; \ddot{x}_g)^T \tag{7}$$

where x_i ($\dot{x}_i$) is the displacement (velocity) of the ith floor relative to the ground, x_m is the displacement of the AMD mass, $\ddot{x}_{ai}$ is the absolute acceleration of the ith floor, and $\ddot{x}_{am}$ is the absolute acceleration of the AMD mass.

Two models of this system are provided, namely an *evaluation* model of the plant, and a *design* model of the plant. The *design* model of the plant is a fairly simple 10 state model of the system, intended to be used in the controller design process (where very high fidelity models are often not available). The *evaluation* model of the plant is a high fidelity 28 state model of the system, which serves as our 'true' representation of the plant. This model is used after the design to evaluate each controller via simulation. The primary goal of the controller design is to provide structural vibration attenuation for this setup during an earthquake. The benchmark problem includes a detailed simulink model to reflect the above setup and constraints, which provides for closed-loop simulation using a pseudo-random disturbance weighted with a Kanai–Tajimi spectrum, and recorded signals from the El Centro and Hachinohe earthquakes. Based on these simulations, a number of additional design constraints on the controller authority, and a set of performance evaluation criteria, J_1–J_{10}, are defined in Reference 1.

4. CONTROLLER SYNTHESIS TECHNIQUES

Consider the general synthesis problem illustrated in Figure 2. In this figure $\mathbf{P} \in \mathscr{RM}$ is the nominal transfer matrix (assumed to be known), and $\mathbf{K} \in \mathscr{RM}$ is the controller (to be designed). The closed-loop system is

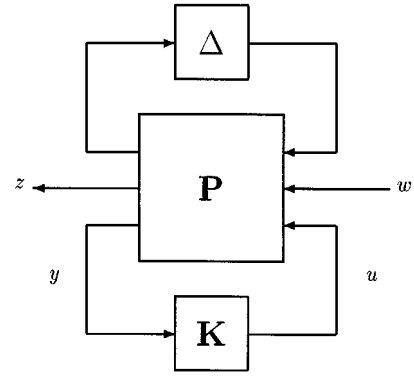

Figure 2. Feedback interconnection for μ synthesis

perturbed by a structured uncertainty $\mathbf{\Delta}$. In this figure the signals w, z, y, u represent exogenous disturbances, error signals, measurements, and control signals respectively. These are vector signals of dimension n_w, n_z, n_y, n_u respectively. The general design problem we will consider is to choose $\mathbf{K}$ so as to meet robust performance, i.e., choose $\mathbf{K}$ so that the perturbed closed-loop system is stable, and the gain from exogenous disturbances (w) to error signals (z) is small, for all allowable $\mathbf{\Delta}$.

We will make the above definition rigorous shortly, but first we would like to make some brief remarks about the motivation for this problem. Note first of all that there is no particular structure imposed on $\mathbf{P} \in \mathscr{RM}$. This gives us a very general problem, and in fact it is easy to rearrange any linear fractional interconnection of systems and uncertainties into the canonical form of Figure 2 by simple block diagram manipulations. In particular, the uncertainty descriptions and performance goals can both be weighted, though not shown as such in Figure 2, since one may simply absorb all the weights into $\mathbf{P}$. There is extensive engineering motivation for this problem, and we refer the interested reader to References 7, 2 and 3 and the references therein.

Since the (complex) uncertainties are typically used to cover unmodelled dynamics, then we wish to be able to consider perturbations which are themselves dynamical systems,with the block diagonal structure of the set $X_{\hat{\mathscr{K}}}$. Associated with any block structure $X_{\hat{\mathscr{K}}}$ let $\mathscr{M}(X_{\hat{\mathscr{K}}})$ denote the set of all real-rational, proper, stable, block diagonal transfer matrices, with block structure like $X_{\hat{\mathscr{K}}}$:

$$\mathscr{M}(X_{\hat{\mathscr{K}}}) \doteq \{\mathbf{\Delta} \in \mathscr{RH}_\infty : \mathbf{\Delta}(\mathbf{j}\omega) \in X_{\hat{\mathscr{K}}} \text{ for all } \omega \in \mathscr{R}\} \tag{8}$$

In this context, we interpret the (complex) uncertainties as the frequency response of any unmodelled dynamics.

Let $\mathbf{T}_{zw}$ denote the transfer matrix from w to z in Figure 2. Our performance goal is to keep the gain of this transfer matrix small (since this is the transfer matrix from disturbance to error) and we will measure this gain as $\|\mathbf{T}_{zw}\|_\infty$. Our robust performance goal can thus be stated rigorously as: *Choose* $\mathbf{K} \in \mathscr{RM}$ *so that the perturbed closed loop system in Figure* 2 *is stable, and* $\|\mathbf{T}_{zw}\|_\infty \leqslant 1$, *for all* $\mathbf{\Delta} \in \mathscr{M}(X_{\hat{\mathscr{K}}})$ *with* $\|\mathbf{\Delta}\|_\infty < 1$.

This problem can be converted into a μ synthesis problem as follows. First, define an augmented uncertainty structure $X_{\mathscr{K}}$ as

$$X_{\mathscr{K}} \doteq \{\text{block diag}(\Delta, \Delta_p) : \Delta \in X_{\hat{\mathscr{K}}},\ \Delta_p \in \mathscr{C}^{n_w \times n_z}\} \tag{9}$$

The perturbation $\mathbf{\Delta}_\mathbf{p}$ is a 'performance block' and by closing the loop from z to w with $\mathbf{\Delta}_\mathbf{p}$ (i.e., let $w = \mathbf{\Delta}_\mathbf{p} z$) the robust performance problem is converted to a robust stability problem, which can be tackled directly with μ. The situation is illustrated in Figure 3.

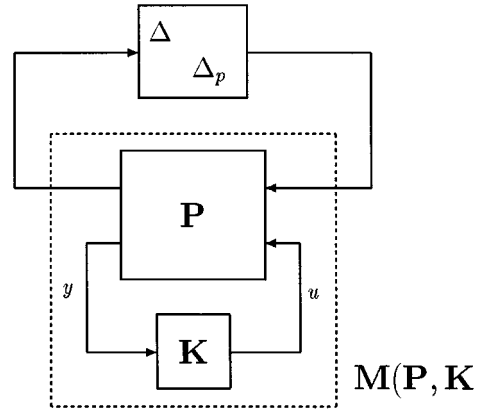

Figure 3. Equivalent robust stabilization problem

We define $\mathbf{M}(\mathbf{P}, \mathbf{K})$ as the nominal closed-loop transfer matrix formed from $\mathbf{P}$ and $\mathbf{K}$ (see Figure 3). To be explicit given any $\mathbf{P}$, $\mathbf{K}$ as above then partition $\mathbf{P}$ in the obvious way as

$$\mathbf{P} = \begin{pmatrix} \mathbf{P}_{11} & \mathbf{P}_{12} \\ \mathbf{P}_{21} & \mathbf{P}_{22} \end{pmatrix} \tag{10}$$

where $\mathbf{P}_{22}$ has n_y outputs and n_u inputs. Then $\mathbf{M}(\mathbf{P}, \mathbf{K})$ is defined by the standard Linear Fractional Transformation formula as

$$\mathbf{M}(\mathbf{P}, \mathbf{K}) \doteq \mathbf{P}_{11} + \mathbf{P}_{12}\mathbf{K}(\mathbf{I} - \mathbf{P}_{22}\mathbf{K})^{-1}\mathbf{P}_{21} \tag{11}$$

With these definitions we have the following well-known robust performance theorem.

Theorem 1. Suppose that the nominal system $\mathbf{M}(\mathbf{P}, \mathbf{K})$ *is stable. Then the perturbed closed-loop system in Figure* 2 *is stable, and*

$$\|\mathbf{T}_{zw}\|_\infty \leqslant 1 \tag{12}$$

for all $\mathbf{\Delta} \in \mathscr{M}(X_{\hat{\mathscr{K}}})$ with $\|\mathbf{\Delta}\|_\infty < 1$ *iff*

$$\sup_{\omega \in \mathscr{R}} \mu_{\mathscr{K}} \mathbf{M}(\mathbf{P}, \mathbf{K})(\mathbf{j}\omega)) \leqslant 1 \tag{13}$$

In light of this result our goal becomes that of the general μ synthesis problem, namely that of finding a controller $\mathbf{K} \in \mathscr{R}\mathscr{M}$ achieving:

$$\inf_{\mathbf{K} \in \mathscr{K}_S} \sup_{\omega \in \mathscr{R}} \mu_{\mathscr{K}}(\mathbf{M}(\mathbf{P}, \mathbf{K})(\mathbf{j}\omega)) \tag{14}$$

where $\mathscr{K}_S$ denotes all $\mathbf{K} \in \mathscr{R}\mathscr{M}$ that render $\mathbf{M}(\mathbf{P}, \mathbf{K})$ internally stable (i.e. the set of *nominally* stabilizing controllers).

4.1. μ Analysis methods

Before considering the μ synthesis problem we first very briefly review the μ analysis problem, i.e. given $M \in \mathscr{C}^{n \times n}$ how does one compute $\mu_{\mathscr{K}}(M)$? In fact, the general analysis problem appears to be computationally intractable (except for small problems or special cases). Nevertheless, approximate computation methods have been developed which rely on readily computable upper and lower bounds (see References 5 and

4 respectively). In this paper we will concentrate on the upper bound, since that actually provides a robustness *guarantee*. The following well-known result is taken from Reference 6.

Theorem 2 (Reference 6). *For any matrix* $M \in \mathscr{C}^{n \times n}$ *and any compatible block structure* $\mathscr{K}$

$$\mu_{\mathscr{K}}(M) \leqslant \inf_{D \in \mathscr{D}_{\mathscr{K}}} \bar{\sigma}(DMD^{-1}) \tag{15}$$

The reason that this upper bound is useful is that it can be computed efficiently. It can be reformulated as a Linear Matrix Inequality (LMI) minimization, and hence a (quasi) convex optimization problem.[5] Efficient software for this bound is now available commercially[8] as part of the μ-Tools Matlab toolbox.[9]

4.2. $\mathscr{H}_\infty$ Optimal control

The $\mathscr{H}_\infty$ optimal control problem can be viewed as a special case of the above μ synthesis problem, where there are *no* uncertainties (i.e. $m = 0$). Thus we have only $\mathbf{\Delta_p}$ (and not $\mathbf{\Delta}$) in Figure 3, and hence only a *nominal* performance (and stability) requirement. The problem thus becomes that of finding a controller $\mathbf{K} \in \mathscr{RM}$ achieving

$$\inf_{\mathbf{K} \in \mathscr{K}_S} \|\mathbf{M}(\mathbf{P}, \mathbf{K})\|_\infty \tag{16}$$

This is illustrated in Figure 4. Note that here, since there are no uncertainties, $\mathbf{M}(\mathbf{P}, \mathbf{K})$ becomes simply the transfer matrix from w to z in Figure 4.

It turns out that finding a (sub) optimal solution to the above is a convex problem, so that the globally optimal controller can be found. The solution was obtained by Doyle *et al*. in Reference 10, and involves the solution of two Riccati equations. Software for computing $\mathscr{H}_\infty$ (sub) optimal controller is now commercially available.[11] This special case can be used to tackle more general problems (and, in particular, the μ synthesis problem), by using an appropriately constructed $\mathbf{P}$ in the above synthesis problem.

4.3. μ Synthesis and D–K iteration

Here we briefly review the μ synthesis problem. For a more detailed exposition see References 12 and 13. As we have already discussed, computing μ is difficult and we are forced to resort to computing bounds. Fortunately, the upper bound is typically very good, and in fact for the type of problems considered here no example with a gap large than 15 per cent (between μ and its upper bound) has been found. Thus, we consider the problem given by replacing μ by its upper bound in equation (14), namely,

$$\inf_{\mathbf{K} \in \mathscr{K}_S} \sup_{\omega \in \mathscr{R}} \inf_{D(\omega) \in \mathscr{D}_{\mathscr{K}}} \bar{\sigma}(D(\omega)\mathbf{M}(\mathbf{P}, \mathbf{K})(\mathbf{j}\omega)D^{-1}(\omega)) \tag{17}$$

Note that if we fix $\mathbf{K}$ then the problem of finding $D(\omega)$ is just the standard μ upper bound problem (across frequency) which is a convex problem and can be efficiently solved. If we choose $D(\omega)$ matrices at a set of

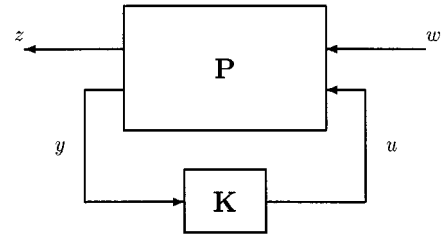

Figure 4. Standard framework for $\mathscr{H}_\infty$ optimal control

frequency points (from the μ upper bound) we can fit a real-rational, stable, minimum-phase transfer matrix to them. If we fix this transfer matrix, $\mathbf{D}$, then the problem of finding $\mathbf{K}$ can be reduced to a standard $\mathscr{H}_\infty$ problem. This is explained in more detail below.

The above approach leads to the following D–K iteration scheme, which attempts to find a μ optimal controller (and hence attempts to optimize robust performance for problems with structured dynamic uncertainty):

Procedure 1 (D–K *Iteration*)

1. *Find an initial estimate of the scaling matrices $D(\omega)$ pointwise across frequency. One possibility is to use the identity matrix at each point.*
2. *Find any state-space realization, $\mathbf{D}_{\text{fit}}$, fitting the pointwise scaling matrices $D(\omega)$ in magnitude. Factor out an all-pass function to yield $\mathbf{D}$ as a stable minimum phase system (so that $\mathbf{D}$ and $\mathbf{D}^{-1}$ are stable) with the same magnitude as $\mathbf{D}_{\text{fit}}$. Augment this with identity matrices as*

$$\mathbf{D}_{\mathbf{L}} \doteq \text{block diag}(\mathbf{D}, I_{n_y}) \quad \mathbf{D}_{\mathbf{R}} \doteq \text{block diag}(\mathbf{D}^{-1}, I_{n_u}) \tag{18}$$

and construct the state-space system

$$\mathbf{P}_{\mathbf{D}} \doteq \mathbf{D}_{\mathbf{L}}\mathbf{P}\mathbf{D}_{\mathbf{R}} \tag{19}$$

so that by construction we have (see Figure 5).

$$\mathbf{M}(\mathbf{P}_{\mathbf{D}}, \mathbf{K}) = \mathbf{D}\mathbf{M}(\mathbf{P}, \mathbf{K})\mathbf{D}^{-1} \tag{20}$$

3. *Find the $\mathscr{H}_\infty$ optimal controller $\hat{\mathbf{K}}$ minimizing $\|\mathbf{M}(\mathbf{P}_{\mathbf{D}}, \mathbf{K})\|_\infty$ over all stabilizing, proper, real-rational controllers $\mathbf{K}$.*
4. *Find $\hat{D}(\omega)$ solving the minimization problem*

$$\inf_{D(\omega)\in\mathscr{D}_{\mathscr{K}}} \bar{\sigma}(D(\omega)\mathbf{M}(\mathbf{P}, \hat{\mathbf{K}})(\mathbf{j}\omega)D^{-1}(\omega))$$

pointwise across frequency.

5. *Compare $\hat{D}(\omega)$ with the previous estimate $D(\omega)$. Stop if they are close, else replace $D(\omega)$ with $\hat{D}(\omega)$ and return to step 2.*

This iteration (assuming perfect state-space realizations of $D(\omega)$) results in $\|\mathbf{M}(\mathbf{P}_{\mathbf{D}}, \mathbf{K})\|_\infty$ being monotonically non-increasing, so that we are guaranteed convergence of the scheme. Having converged then the controller $\hat{\mathbf{K}}$ from step 3 is the resulting μ synthesis controller. Note that although the individual problems (the μ upper bound and $\mathscr{H}_\infty$ optimal control) are convex, the joint problem is not convex (see Reference 12 for a counterexample to convexity). Thus the D–K iteration described above is not guaranteed to converge to

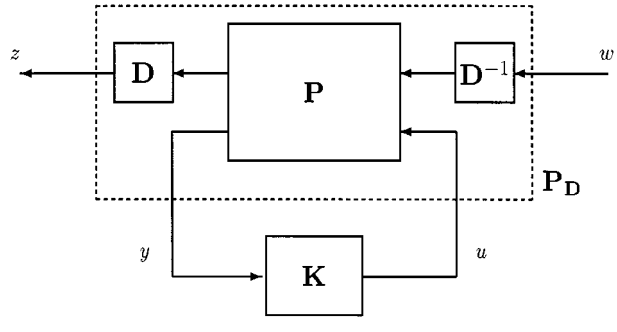

Figure 5. D–K Iteration as an $\mathscr{H}_\infty$ optimal control problem

the global optimum of equation (17), and in fact it may converge to a saddle point of the problem which is not even a *local* minimum (with respect to D and K *jointly*). However, many designs have been performed using this technique in recent years (see References 14 and 15 for example), and it has usually been found to work well in practice. There are further subtleties to the above procedure, which we will not go into here (see References 13 and 9 for more details).

This D–K iteration scheme is the basis of μ synthesis controller design. The design process consists essentially of the following stages.

Procedure 2 (μ *Synthesis*)

1. *Decide on an appropriate interconnection structure to model the system, including the uncertainty structure against which robustness is desired.*
2. *Choose appropriate weights to reflect the desired performance specifications, and any information known about the uncertainties.*
3. *Implement the above* D–K *iteration. Note that this involves deciding on an appropriate frequency range of interest, and selecting the order of the State Space fit in step* 2.

This procedure is by no means mechanical, and a good deal of engineering judgement is still required, particularly in steps 1 and 2. Also, as with any control design technique, the full design process may well involve an iterative application of the above process, together with an evaluation of each resulting controller.

4.4. Controller order reduction and balanced truncation

Having obtained a design, it is often desirable, for numerical and implementation reasons, to reduce the number of states in the controller. Here we very briefly review the balanced truncation technique for controller order reduction. For a more detailed treatment we refer the interested reader to Reference 16. For a stable state-space system $\mathbf{K}$,

$$\mathbf{K} = \left[\begin{array}{c|c} A_k & B_k \\ \hline C_k & D_k \end{array}\right] \tag{21}$$

the controllability (P) and observability (Q) grammians are defined as the solutions of the following Lyapunov equations:

$$\begin{aligned} A_k P + P A_k^{\mathrm{T}} + B_k B_k^{\mathrm{T}} &= 0 \\ A_k^{\mathrm{T}} Q + Q A_k + C_k^{\mathrm{T}} C_k &= 0 \end{aligned} \tag{22}$$

A balanced realization is a state-space representation in which these Grammians are equal and diagonal:

$$P = Q = \Sigma = \mathrm{diag}(\sigma_1, \ldots, \sigma_{n_k}) \tag{23}$$

where n_k is the order of $\mathbf{K}$. In light of this, the above Hankel Singular Values (HSV), σ_i, of the system represent the degree to which each state is both controllable and observable. Hence, we may delete states whose HSV is small to produce a reduced-order model $\mathbf{K}_{\mathrm{red}}$, whose input–output properties should not differ greatly from $\mathbf{K}$. In fact, it can be shown that if the σ_i are in decreasing order, and we delete the smallest $(n_k - n_{\mathrm{red}})$ balanced states (so that $\mathbf{K}_{\mathrm{red}}$ is of order n_{red}) then we are guaranteed that

$$\|\mathbf{K} - \mathbf{K}_{\mathrm{red}}\|_\infty \leqslant 2 \sum_{i = n_{\mathrm{red}} + 1}^{n_k} \sigma_i \tag{24}$$

Thus, one choice for model reduction is to first employ a state space similarity transformation to yield a balanced realization of the system, and then truncate this system by deleting the undesirable states. This process is referred to as balanced truncation.

5. APPLICATION TO THE BENCHMARK PROBLEM

The benchmark problem provides us with a model of the open-loop plant, including models for the sensors and actuator. In order to apply the μ synthesis design technique to the benchmark problem, we first need to decide on the design system interconnection. This will specify:

1. What uncertainties are present in the system?
2. Which disturbance signals act on the system?
3. Which signals do we wish to penalize in the optimal control problem?
4. What measurements will the controller use?

After several design iterations, we came up with the interconnection shown in Figure 6, where the signals $\hat{z}$, $\hat{y}$ are given as

$$\hat{z} = (d_1 \;\; d_2 \;\; d_3 \;\; \ddot{x}_{a1} \;\; \ddot{x}_{a2} \;\; \ddot{x}_{a3} \;\; x_m \;\; \dot{x}_m \;\; \ddot{x}_{am})^T \tag{25}$$

$$\hat{y} = (\ddot{x}_{a1} \;\; \ddot{x}_{a2} \;\; \ddot{x}_{a3} \;\; \ddot{x}_{am})^T \tag{26}$$

The above four questions are addressed in the selection process for the design interconnection structure, as follows:

1. The design includes two uncertainties. Firstly there is additive uncertainty, $\mathbf{\Delta}_a$, on the plant model. Note that the *design* model is obtained via a model reduction procedure on a higher-order *evaluation* model, which is a more accurate representation of the true system (see Reference 1 for details). Thus, we clearly

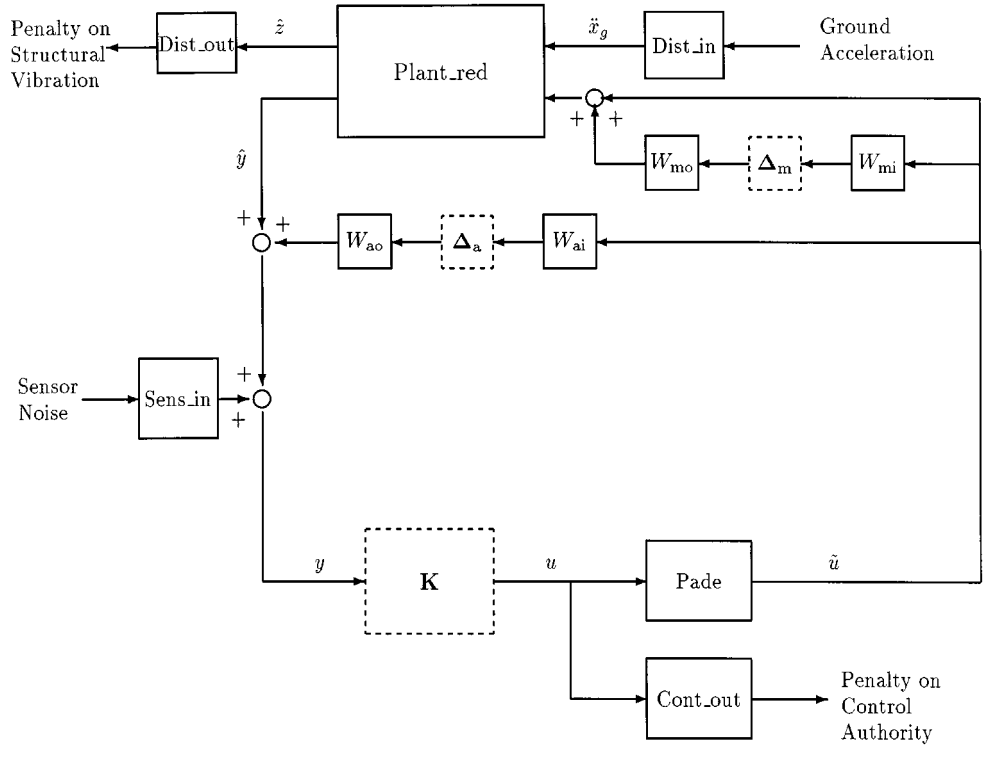

Figure 6. Interconnection for μ synthesis design

need this uncertainty to account for unmodelled dynamics, particularly at high frequency. However, it is important to note that some uncertainty of this type would always be required for a robust design, even if we used the more accurate model, because no model will exactly capture the behaviour of the true system. We also include some multiplicative uncertainty, $\mathbf{\Delta}_m$, on the AMD, to account for deficiencies in the actuator model. These uncertainty descriptions are very important in the design process, to prevent the optimal control design from being too aggressive. This can lead to controllers which exploit the model properties to such an extent that they perform very well in simulation, but not at all well on the actual system. For the benchmark problem an attempt to capture this effect is made by using the low-order *design* model of the plant for controller synthesis, and a more accurate *evaluation* model of the plant for the simulations.

2. The choice of disturbance signals for the design is fairly natural. Clearly, we wish to consider the ground acceleration due to the earthquake as one disturbance signal. In any meaningful problem there is always sensor noise present, and so we also include this as a disturbance signal. Note also that without the sensor noise disturbance one has a singular control problem, which leads to numerical difficulties.
3. The choice of which signals to penalize is also fairly natural. The performance criteria for the benchmark problem are all specified in terms of the nine signals d_1, d_2, d_3, $\ddot{x}_{a1}$, $\ddot{x}_{a2}$, $\ddot{x}_{a3}$, x_m, $\dot{x}_m$, $\ddot{x}_{am}$, which correspond to inter-storey drift on each floor, absolute acceleration of each floor, and the displacement/velocity/acceleration of the AMD system. Thus, we wish to penalize these signals, hence the (weighted) penalty on $\hat{z}$. In addition, for any control design we always wish to limit the control authority, and so we include a (weighted) direct penalty on the control signal, u. Again, this is desirable from a numerical viewpoint to avoid a singular control problem.
4. The choice of measurements to use in the controller is more difficult. We did not use the pseudo-velocity measurements since, from an optimal viewpoint, these signals provide no additional information content (they are merely filtered versions of signals the controller already has access to). Our goal was to only use the accelerometer measurements from each floor and from the AMD, $\ddot{x}_{a1}$, $\ddot{x}_{a2}$, $\ddot{x}_{a3}$, $\ddot{x}_{am}$, since these are measurements that one could reasonably expect to have available in a (full-scale) field setup. However, the initial designs were performed using also the ground acceleration and AMD displacement $\ddot{x}_g$, x_m, so as to determine the best control design we could provide. Having obtained this design, we determined that the controller gains for these two measurements were the least significant, which suggested that one could obtain similar performance without using them. Thus, the controller was redesigned using only the four accelerometer measurements, $\hat{y}$, in Figure 6. This final design provided almost the same level of performance as the initial design using all the available measurement information. This illustrates one of the advantages of an optimal controller synthesis procedure. Not only were we able to come up with a design using a small number of measurements, but we could also quantify the loss in performance resulting from not using all the measurements. This loss was acceptably small. An analysis of the final design showed that all the controller gains were significant, so we would expect some degradation in performance if we tried to use even fewer measurements. Since we had already met our goal in this regard, we did not attempt any further reduction in the measurements.

The interconnection system shown in Figure 6 includes the following elements:

Transfer matrices:

Plant_red: This is the nominal transfer matrix of the system from ground acceleration and (delayed) control input, $\ddot{x}_g$, $\tilde{u}$, to the penalty signals and measurements $\hat{z}$, $\hat{y}$. It is straightforward to obtain this model from the *design* model of the plant provided in the benchmark problem (yielding Plant_red with 10 states, 13 outputs, and 2 inputs).

Pade: This system is given as

$$\text{Pade} = \frac{-s + 10^4}{s + 10^4} \tag{27}$$

and is a first order Pade approximation to a time delay of 200 μs, included to account for the computation time required by the DSP controller.

Weights:

W_{ao}, W_{ai}: These weights were chosen based largely on the difference between the *evaluation* and *design* plant models, so that the additive uncertainty could account for unmodelled dynamics in the system.

$$W_{ao}(s) = \frac{13s^2 + 243{\cdot}4s + 2637}{s^2 + 71{\cdot}3s + 2623{\cdot}4} \tag{28}$$

$$W_{ai} = 0{\cdot}01I_6 \tag{29}$$

W_{mo}, W_{mi}: These weights were simply chosen to include 0·2 per cent actuator uncertainty:

$$W_{mo} = \sqrt{0{\cdot}02} \tag{30}$$

$$W_{mi} = 0{\cdot}1\sqrt{0{\cdot}02} \tag{31}$$

Dist_in: This weight was chosen to reflect the frequency content of the Kanai–Tajimi power spectral density

$$\text{Dist\_in}(s) = \frac{\sqrt{S_0}(2\zeta_g\omega_g s + \omega_g^2)}{s^2 + 2\zeta_g\omega_g s + \omega_g^2} \;\Rightarrow\; |\text{Dist\_in}(\mathbf{j}\omega)|^2 = \frac{S_0(4\zeta_g^2\omega_g^2\omega^2 + \omega_g^4)}{(\omega^2 - \omega_g^2)^2 + 4\zeta_g^2\omega_g^2\omega^2} \tag{32}$$

Worst-case values were selected as $S_0 = 0{\cdot}1$, $\zeta_g = 0{\cdot}3$, $\omega_g = 37{\cdot}3$ rad/s.

Dist_out: This weight can be used to vary the penalty placed on each of the nine signals in $\hat{z}$. Our performance goal was to have each of the performance indices $J_1 - J_{10}$ below one. These goals relate naturally to the signals in $\hat{z}$, and hence the weights in Dist_out. After a number of design iterations our final weight selection was:

$$\text{Dist\_out} = \text{diag}(0{\cdot}002,\ 0{\cdot}0015,\ 0{\cdot}001,\ 0{\cdot}01,\ 0{\cdot}015,\ 0{\cdot}02,\ 0{\cdot}0004,\ 0{\cdot}055,\ 0{\cdot}2) \tag{33}$$

Sens_in: These weights are chosen to reflect 1 per cent sensor noise in each measurement:

$$\text{Sens\_in} = \text{diag}(0{\cdot}02,\ 0{\cdot}03,\ 0{\cdot}04,\ 0{\cdot}04) \tag{34}$$

Cont_out: This weight was chosen to penalize the use of large control signals. Cont_out is a high-pass filter (see Figure 7 for a Bode magnitude plot) which places a very high penalty on signals above 35 Hz (220 rad/s). This ensures that the controller rolls off adequately at high frequencies (so as not to excite high-frequency modes), and does not require excessive bandwidth.

$$\text{Cont\_out}(s) = \frac{0{\cdot}55s + 13{\cdot}62}{s + 285{\cdot}1} \tag{35}$$

This design interconnection results in a **P** (see Figure 2) with 16 states, 16 outputs and 11 inputs. The uncertainty structure is given as

$$X_{\mathscr{K}} = \{\text{block diag}(\mathbf{\Delta}_a, \mathbf{\Delta}_m, \mathbf{\Delta}_p)\colon \mathbf{\Delta}_a \in \mathscr{C}^{4\times 1},\ \mathbf{\Delta}_m \in \mathscr{C}^{1\times 1},\ \mathbf{\Delta}_p \in \mathscr{C}^{5\times 10}\} \tag{36}$$

with four measurements in y and one control signal in u. The D–K Iteration for controller synthesis outlined in Section 4.3 was carried out for this interconnection. It was found that constant D-scales were adequate for the design, so the resulting μ synthesis controller was 16th order. This design yielded a peak value for μ across

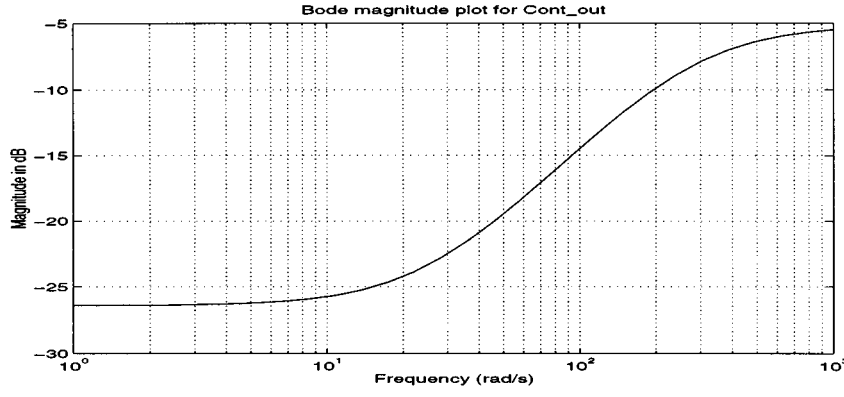

Figure 7. Bode magnitude plot for Cont_out

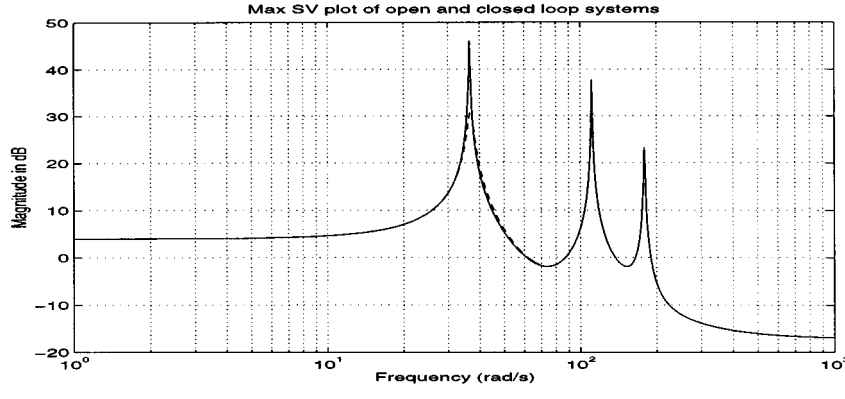

Figure 8. $\bar{\sigma}(T(\mathbf{j}\omega))$ for the open-(solid) and closed-(dashed) loop systems

frequency of 0·88, and $\mu_{\mathscr{K}}(\mathbf{M}(\mathbf{P}, \mathbf{K})(\mathbf{j}\omega))$ is plotted in Figure 9. Note that the robust performance is dominated by the first mode of the structure at 36·5 rad/s, and μ is very small away from this frequency. Thus, it appears that the performance specifications for this problem are dominated by the need to get good control of the first vibration mode of the structure. This is confirmed by examining the plot in Figure 8, which shows $\bar{\sigma}(T(\mathbf{j}\omega))$ plotted against frequency, for both the open- and closed-loop systems. Here $T(s)$ is the transfer matrix from $\ddot{x}_g$ to $(d_1\ d_2\ d_3\ \ddot{x}_{a1}\ \ddot{x}_{a2}\ \ddot{x}_{a3})^T$. Thus, it represents the gain from the ground excitation to the vibration of the structure. It is clear that the controller provides large attenuation of the first mode at 36·5 rad/s, some attenuation of the second mode at 111 rad/s, and little effect on any higher-order modes.

The fact that the peak value of μ across frequency is less than one means that we have met all our robust performance goals. Furthermore, since μ is very small above 50 rad/s, we have a very high degree of robustness to any uncertainties in the higher-order modes.

Note that the solution of the $\mathscr{H}_\infty$ optimal control problem always returns a controller of the same order as the design interconnection, and hence (if we include D-scales) so does μ synthesis. However, many of the controller states may be operating at high frequency, and hence contributing very little to the performance. Examining the Hankel Singular Values of this controller revealed that only the first three were significant, and so the balanced truncation procedure outlined in Section 4.4 was used to reduce to a third-order

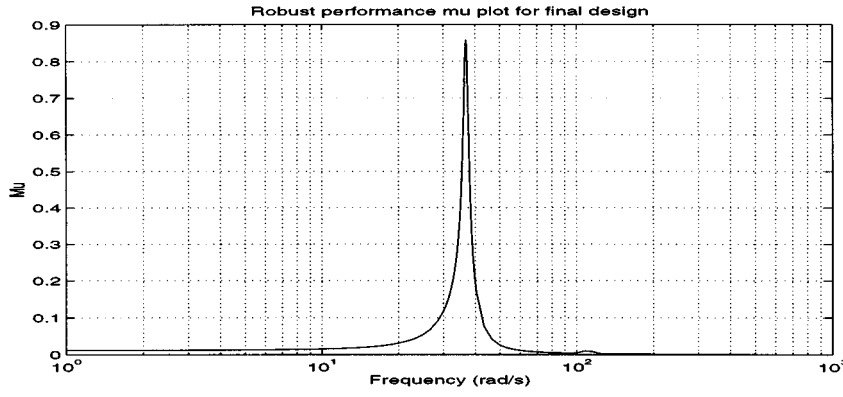

Figure 9. Robust performance μ plot

controller. Repeating the above μ analysis with this controller revealed a negligible increase in the peak value of μ, and hence a negligible loss of robust performance.

The final stage of the design was to convert this continuous-time controller to a discrete-time controller operating at 1 kHz, by implementing a bilinear transformation. Note that the effects of a discrete-time implementation of the controller have already been accounted for in the design process, by the use of the Pade approximation to the computation time delay.

6. RESULTS AND DISCUSSION

We chose a performance goal for our design of keeping all the performance measures J_1–J_{10} below one (note that this requirement is not met by the $\mathscr{H}_2$ optimal control design example provided in Reference 1, because of the difficulty of keeping J_{10} small). The results from running the supplied simulation model (which uses the full order *evaluation* model of the plant, and implements some constraints on the controller in terms of sampling-time/computation delay, A/D and D/A precision/range, and sensor noise) are tabulated in Table I. Note that J_1–J_5 were calculated using $\zeta_g = 0{\cdot}3$, $\omega_g = 37{\cdot}3$ rad/s, and averaging over a 300 s time period. For J_6–J_{10} the Hachinohe earthquake was the limiting value in each case, and the corresponding value for the El Centro earthquake is given in parentheses.

It can be seen that this design meets our goals. If we consider group 1 of the measures as J_1, J_2, J_6, J_7, then these correspond to the structural vibration attenuation of the system, and hence lower numbers here correspond to smaller interstorey drift and absolute acceleration of the bays of the structure. Group 2 of the measures, J_3–J_5 and J_8–J_{10}, corresponds to the displacement/velocity/acceleration of the AMD system. Thus, these values reveal the control effort we expend. It is clear that there is a natural tradeoff between group 1 (vibration attenuation) and group 2 (control effort) of the measures, and we would expect that the control designer can reduce the numbers in group 1 at the expense of increasing those in group 2. Indeed this is the case and it is fairly easy to produce an array of designs, whereby vibration attenuation is traded off against control effort, by varying the weight selection in the design interconnection in Figure 6. For reasons of brevity we do not include the details here.

This controller design meets all of the constraints. It is a third-order discrete-time controller (operating at 1 kHz), which is itself stable, and it stabilizes the closed-loop system (both verified by eigenvalue analysis). The peak/allowed values for various signals obtained from the above simulations are tabulated in Table II.

Note that this design is not very aggressive, since it easily passes all the required constraints, with the largest value being 60 per cent of the allowed maximum for $\ddot{x}_{am}$ for the El Centro earthquake. In light of this it seems likely that we could obtain better vibration attenuation for this problem with a more aggressive design.

Table I. Performance measures for the final design

J_1	0·244	J_6	0·406 (0·389)
J_2	0·376	J_7	0·730 (0·591)
J_3	0·638	J_8	0·983 (0·868)
J_4	0·636	J_9	0·999 (0·821)
J_5	0·570	J_{10}	0·754 (0·714)

Table II. Performance constraints for the final design

	Kanai-Tajimi			Hachinohe			El Centro		
Constraint	RMS	Allowed	%	Max	Allowed	%	Max	Allowed	%
u	0·21	1	21	0·45	3	15	0·83	3	28
x_m	0·84	3	28	1·63	9	18	2·93	9	33
$\ddot{x}_{am}$	1·02	2	51	1·95	6	32	3·60	6	60

Indeed we were able to produce designs with significantly higher performance, at the expense of increased control effort (we do not include them here for reasons of brevity). Note however that this increases the performance measures in group 2 (control effort), and our stated goal was to keep all the measures below one.

The continuous-time version of the controller is given in state-space form as

$$\mathbf{K} = \left(\begin{array}{rrr|rrrr} -9{\cdot}6293 & 28{\cdot}6195 & -14{\cdot}1659 & 0{\cdot}5983 & 0{\cdot}8746 & 1{\cdot}2081 & -0{\cdot}5156 \\ -28{\cdot}4550 & -10{\cdot}9452 & 27{\cdot}0656 & 0{\cdot}6523 & 0{\cdot}6011 & 0{\cdot}8082 & -0{\cdot}4113 \\ 8{\cdot}0171 & -14{\cdot}2982 & -10{\cdot}0320 & -0{\cdot}1379 & -0{\cdot}4698 & -0{\cdot}3309 & -0{\cdot}8106 \\ \hline 1{\cdot}6877 & -1{\cdot}2685 & 1{\cdot}0031 & 0 & 0 & 0 & 0 \end{array}\right) \tag{37}$$

Note that it is strictly proper and stable. The Bode plots for the controller are given in Figure 10, which shows that each of the (four) controller gains is significant. This controller was designed to be robust, as verified by the μ plot in Figure 9. As a result, the controller gains appear well behaved, with no sharp resonances, and all the gains roll off well before 35 Hz (220 rad/s) so that the controller bandwidth is not excessive. The robustness of this design is best verified via a μ plot as discussed earlier, but in order to facilitate comparison with other approaches the benchmark robustness test suggested in Reference 1 was also carried out. The loop gain transfer function is plotted in Figure 11, and the suggested criterion is that it should remain below -5 dB above 35 Hz (220 rad/s). It can be seen that the design easily meets this robustness criterion, and in fact the loop gain remains below -25 dB for frequencies above 35 Hz (220 rad/s).

It appears that the μ synthesis procedure is an effective design approach for this problem. We are able to provide a simple linear controller, which is low order with small required bandwidth, has excellent robustness properties, and meets all of the design constraints, using only the four accelerometer measurements. Furthermore, it delivers decent performance with good vibration attenuation for only modest control effort, so that our criterion of keeping J_1–J_{10} all below one was met. The performance tradeoff could easily be varied to yield a more/less aggressive design as desired. The design was performed using commercially available software, and the computational requirements were not excessive. Designs using this approach can readily be performed in a reasonable time using a PC.

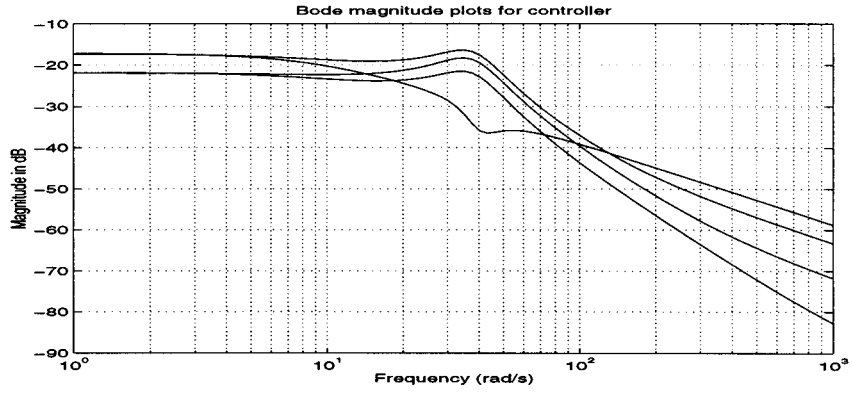

Figure 10. Bode magnitude plots for controller

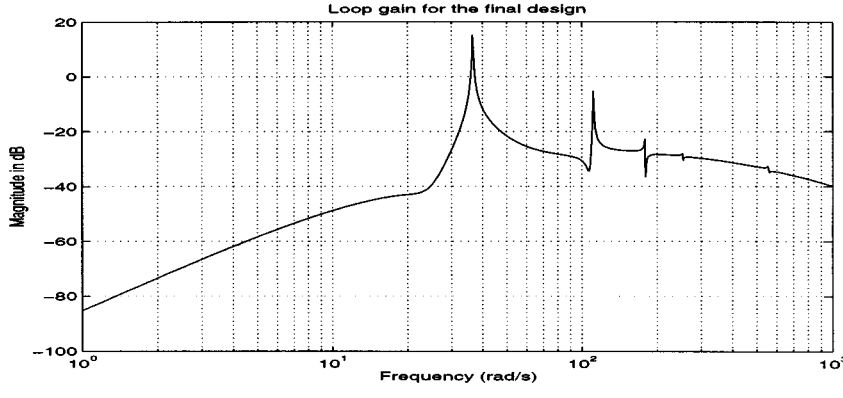

Figure 11. Loop gain for the final design

7. CONCLUDING REMARKS

This problem placed high-performance requirements on the first mode of the structure, together with robustness requirements on the higher-order modes. Robust designs are required so as to avoid spillover problems, which are an important consideration in controller design for civil engineering applications. At the same time the controller should use limited actuator authority, and satisfy certain implementation constraints typical of a practical setting. We found the μ synthesis procedure for robust controller design to be an excellent vehicle for studying these tradeoffs in a systematic fashion, and we were able to design a simple controller which met the above requirements. The controller had a low order, and a small required bandwidth, both of which are desirable properties often lacking in optimal control designs.

REFERENCES

1. B. F. Spencer Jr., S. J. Dyke and H. S. Deoskar, 'Benchmark problems in structural control: Part I—Active mass driver system', *Earthquake Engng. Struct. Dyn.* **27**, 1127–1139 (1998).
2. P. M. Young, M. P. Newlin and J. C. Doyle, 'μ analysis with real parametric uncertainty', *Proc. 30th Conf. Decision and Control*, 1991, pp. 1251–1256.

3. P. M. Young, Robustness with parametric and dynamic uncertainty, *Ph.D. thesis*, California Institute of Technology, 1993.
4. P. M. Young and J. C. Doyle, 'Computation of μ with real and complex uncertainty', in *Proc. 29th Conf. Decision and Control*, 1990, pp. 1230–1235.
5. M. K. H. Fan, A. L. Tits and J. C. Doyle, 'Robustness in the presence of mixed parametric uncertainty and unmodeled dynamics', *IEEE Trans. Automat. Control* **36**, 25–38 (1991).
6. J. C. Doyle, 'Analysis of feedback systems with structured uncertainty', *IEE Proc.*, Part D **129**, 242–250 (1982).
7. A. K. Packard and J. C. Doyle, 'The complex structured singular value', *Automatica* **29**, 71–109 (1993).
8. P. M. Young, M. P. Newlin and J. C. Doyle, 'Practical computation of the mixed μ problem', *Proc. American Control Conf.*, 1992, pp. 2190–2194.
9. G. J. Balas, J. C. Doyle, K. Glover, A. K. Packard and R. S. Smith, 'The μ analysis and synthesis toolbox', MathWorks and MUSYN, 1991.
10. J. C. Doyle, K. Glover, P. Khargonekar and B. A. Francis, 'State space solutions to $\mathscr{H}_2$ and $\mathscr{H}_\infty$ control problems', *IEEE Trans. Automat. Control* **34**, 831–847 (1989).
11. G. J. Balas, A. K. Packard, J. C. Doyle, K. Glover and R. Smith, 'Development of advanced control design software for researchers and engineers', *Proc. American Control Conf.*, 1991, pp. 996–1001.
12. J. C. Doyle, 'Structured uncertainty in control system design', *Proc. 24th Conf. on Decision and Control*, 1985, pp. 260–265.
13. G. Stein and J. C. Doyle, 'Beyond singular values and loop shapes', *J. Guidance, Control Dyn.* **14**, 5–16 (1991).
14. G. J. Balas, C. Chu and J. C. Doyle, 'Vibration damping and robust control of the JPL/AFAL experiment using μ-synthesis', *Proc. 28th Conf. on Decision and Control*, 1989, pp. 2689–2694.
15. G. J. Balas and J. C. Doyle, 'Robustness and performance tradeoffs in control design for flexible structures', *Proc. 29th Conf. on Decision and Control*, 1990, pp. 2999–3010.
16. K. Zhou, J. C. Doyle and K. Glover, *Robust and Optimal Control*, Prentice-Hall, Englewood Cliffs, New Jersey, 1996.

